CHAPTER 5

Plume, Signal Interference and Plume Signature

GÉRARD PRIGENT

1. Introduction

The presence of a plume with attendant radiation and smoke at the aft end of a missile, due to the combustion and pyrolysis products of the rocket motor exhausted through the nozzle, may cause a missile to fail in its mission.

The plume or smoke may reveal the launch location of a missile and allow the missile to be located in flight. In the case of missiles guided optically (at visible or infrared wavelengths), the transmission of commands through the plume or smoke trail may be substantially attenuated, leading to the loss of control of the missile. Intense flames at the rear of the missile, caused by combustion of the motor exhaust products with air (afterburning), may also reveal the launcher location and trajectory of the missile.

The flames may also cause saturation of the instruments used for optical tracking of the missile or of the target. The flames increase the temperature of the plume, resulting in increased emission of infrared radiation. In addition, the transmission of radar frequency electromagnetic waves is generally very weakened by absorption by these flames that contain ionized species. The flames have also been known to cause engine flameout of jet aircraft that launch the missiles, and also damaging impingement effects on launcher surfaces.

Finally, the nozzle exhaust products may often cause a disturbance of the thrust vector control components because of slag or erosion.

The principal methods used to guide and control missiles [1,2] new ref usually require links between:

- the firing station and the missile;
- the firing station and the target;
- the missile and the target.

TABLE I *Major co*...

Composition	HCl
EDB	0
Smokeless EMCB (NC, Ngl, RDX)	0
Butalite (HTPB + AP)	17
Butalane	16

ᵃ Molar fractions inside the cha...
ᵇ Combustion temperature insi...
ᶜ Total fraction of the conden... expansion.

This value, always so... the composition of the ...

Assuming that the ga... thermodynamic equilibri...

is sufficient to provide an ... the mixture's principal in... used as examples in Ta... propellants it decreases w... it increases with the level... propellants it usually va... perature. When the mixi... accompanied by afterbur... ture, increase significantl...

2.3. PRIMARY SMOKE

Primary smoke consist... exhausted at the exit pla... because it exhibits the tri... and scattering ultraviolet... optical magnitudes depen...

The smoke may come... insulation, or from any o... the combustion gases, as ...

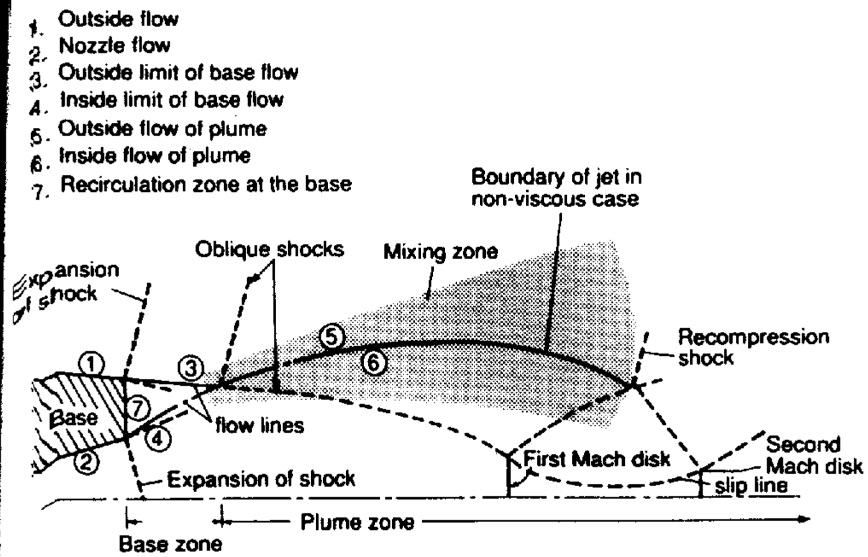

FIG. 5.1. Diagram of the zones of the plume of missile in flight.

Condensed exhaust products, solid or liquid, may be present downstream of the nozzle exit plane, leading to the presence of plume smoke, called primary smoke. Secondary smoke may develop, further downstream and in external regions of the plume, depending on the atmospheric conditions, caused by the condensation of water vapor from both the plume and the atmosphere.

The attenuation of radar waves and infrared emissions are more important in the plume, and the absorption and scattering of visible light are more important in the smoke trail.

Most of the chemical products in the plume come from combustion of the propellant. Additional contributions to the exhaust gases and particles come from thermal and mechanical erosion, pyrolysis and combustion of the inhibitors, liners and insulators, and from ablation of nozzle and blast-tube materials.

2.2. THE GASEOUS PRODUCTS

The major gaseous products contained in the combustion residue mixture are nearly always CO, CO_2, H_2, H_2O and N_2. Propellants containing ammonium perchlorate produce, in addition, hydrochloric acid HCl (Table 1).

The reducing power or fuel index of a gaseous mixture is usually characterized by the sum of molar fractions of hydrogen H_2 and of carbon monoxide CO.

$$P = N_{CO} + N_{H_2}$$

TABLE 1 *Major combustion products from typical propellants calculated*

Composition	N%[a] HCl	CO	CO_2	H_2	H_2O	N_2	Condensed products[c]	T^b(K)
EDB	0	38	13	10	23	12	1.5	2630
Smokeless EMCB (NC, Ngl, RDX)	0	34	12	10	23	19		2775
Butalite (HTPB + AP)	17	18	8	12	36	9	0.2	2798
Butalane	16	22	1.3	31	11	8	10	3620

[a] Molar fractions inside the chamber.
[b] Combustion temperature inside the chamber.
[c] Total fraction of the condensed particles at the exit plane of the nozzle after equilibrium expansion.

This value, always somewhere between 0 and 1, is obtained by analyzing the composition of the gases inside the combustion chamber (Chapter 3).

Assuming that the gaseous mixture in the combustion chamber is in thermodynamic equilibrium, the reaction

$$CO + H_2O \underset{(2)}{\overset{(1)}{\rightleftarrows}} CO_2 + H_2$$

is sufficient to provide an initial approximation to the respective amounts of the mixture's principal ingredients. The reducing power of the few propellants used as examples in Table 1 ranges from 0.3 and 0.55. With composite propellants it decreases when the ammonium perchlorate level increases, and it increases with the level of HMX and aluminium. With EDB and CMDB propellants it usually varies conversely with the combustion chamber temperature. When the mixing of the combustion residual products with air is accompanied by afterburning, the level of CO_2 and H_2O and the temperature, increase significantly.

2.3. PRIMARY SMOKE

Primary smoke consists of a mixture of liquid and solid particles usually exhausted at the exit plane with the combustion gases. It is easily detected because it exhibits the triple capacity of, at the same time, absorbing, emitting and scattering ultraviolet, visible, or infrared radiation. The corresponding optical magnitudes depend on the number, size and nature of the particles.

The smoke may come from the pyrolysis of the inhibitor, the thermal insulation, or from any other parts of the motor that come into contact with the combustion gases, as well as from the propellant itself, which may contain

ballistic catalysts, anti-instability additives, and flash suppressors with mineral elements or reducing metallic fuel solids. It may also sometimes originate directly in the combustion chamber as in the case of alumina, which is liquid at a temperature over 2315 K, or of zirconium oxide, which solidifies as soon as the temperature drops below 2990 K.

Other chemical products condense further beyond the throat of the nozzle. Lead, copper, potassium and their oxides, for example, produce submicron-size particles. From an attenuation point of view, these particle sizes result in absorption and scattering of visible and infrared light which are very notable.

Carbon and soot particles constitute a special case. They are primarily caused by the pyrolysis of materials of the chamber (liners, insulators, etc.). Their size increases as a function of the residence time in the combustion chamber [4]. Their size at the nozzle exit remains small, between 10^{-1} and 10^{-2} μm, contributing significantly to the signature of the plume, particularly at shorter wavelengths.

End-burning grains that are inhibited on the lateral face produce a significant amount of this type of primary smoke. It has been demonstrated that the polyester inhibitor, having lost 3% of its mass due to heating by the combustion gases of a CDB propellant (reducing power 0.6, combustion temperature 2000 K) is enough to produce 1% (in mass) of soot in the smoke. This quantity is sufficient to make the smoke trail of a missile detectable.

2.4. SECONDARY SMOKE

The combustion of propellant containing ammonium perchlorate (Butalite, reduced smoke Nitramite) produces hydrochloric gas. Under specific atmospheric conditions of temperature and humidity (Fig. 2) the combination with air results in the formation of a mist of azeotropic liquid drops of H_2O and HCl.

It is observed that it usually takes several seconds for the secondary smoke cloud to reach maximum opacity (Fig. 3). Increases of the absorption and scattering of the visible and infrared light occur simultaneously, due to the growth both in number and size of the drops.

In the case of composite propellants, with ammonium perchlorate contents greater than 60%, the secondary smoke forms a very dense fog.

In contrast, the smoke observed during the firing of a XLDB (high-energy binder + HMX) propellant with a low ammonium perchlorate percentage is translucent, and difficult to differentiate from the primary smoke due to some additives.

The importance of the secondary smoke depends on the operational climatic environment of the missile. Table 2 compares the frequency of the occurrence of secondary smoke for two propellants based on climate variations (according to statistics provided by the French National Weather Bureau).

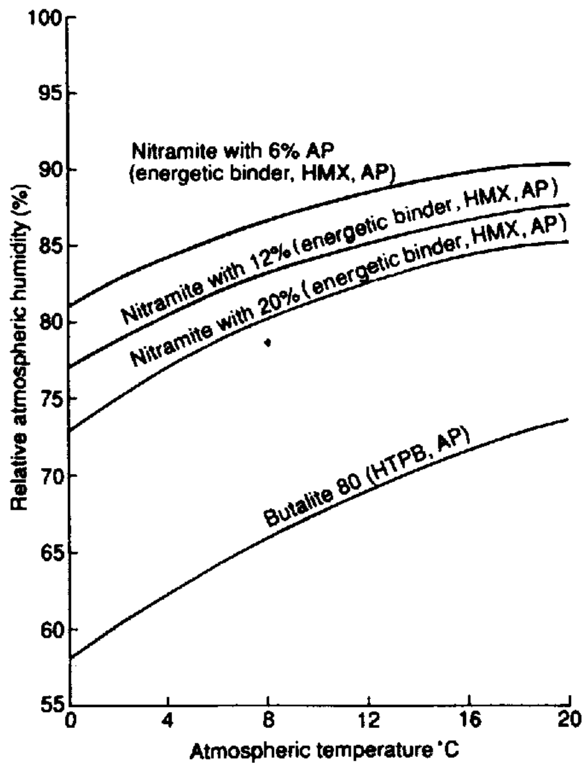

FIG. 5.2. Range of occurrence of secondary smoke.

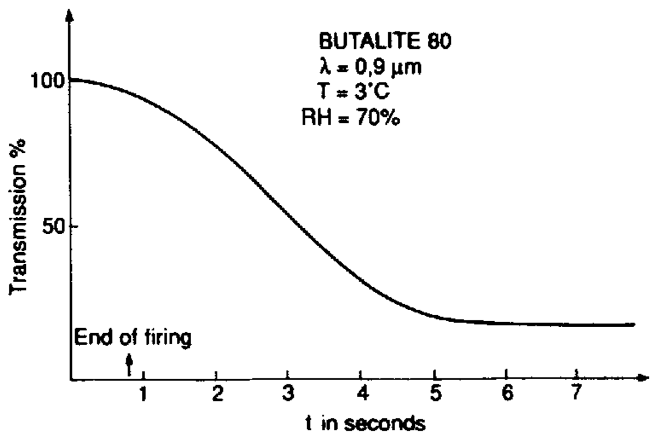

FIG. 5.3. Growth kinetics of a trail of secondary smoke in a climatic chamber ($600\ m^3$). Transmission versus time.

TABLE 2

Season	Frequency of occurrence of secondary smoke in Paris Montsouris (percentages)	
	82% AP composite	15% AP XLDB
Spring	30	17
Summer	19	4
Fall	50	25
Winter	64	40
Annual average	40	21

2.5. PLUME AFTERBURNING

Since the specific impulse of a propellant is inversely proportional to the square root of the molecular weight of the gases, it is more efficient, from the standpoint of thrust, to select a fuel-rich propellant whose combustion produces an underoxidized (less than stoichiometric) gaseous mixture with more carbon monoxide molecules than carbon dioxide, and more hydrogen than water, and thus a relatively high reducing power. Theoretically, we note the reducing power varies relatively little during the expansion through the nozzle, so that downstream of the exit plane the gases are likely to burn again when they mix with atmospheric oxygen. This phenomenon is called afterburning or secondary combustion of the plume.

The motor exhaust flow, the design of the base of the missile, the speed of the missile, the altitude, the pressure of the combustion chamber, and the expansion ratio of the nozzle exit plane are some of the variables that, like the reducing power and the temperature of the gases, affect the probability that afterburning will occur, and at the same time, influence the ignition point and the position of the flame in the exhaust flow downstream of the nozzle.

Afterburning is a complex phenomenon, and its parametric study is made very difficult because the influence of the various parameters is not additive, and because of their interactions within a complicated flowfield, typified by Fig. 1.

Afterburning causes a temperature increase in the plume with resulting increases in luminosity, infrared emission, concentration of ions and free electrons (which increases radar attenuation and radar cross-section). Afterburning also increases the turbulence of the plume and, consequently, the interference and defocusing of guidance laser beams, and the noise imposed on radar guidance signals. The acoustic noise of a rocket motor is also increased by afterburning. Afterburning may also modify the nature and quantity of primary and secondary smoke.

Because of the very high temperatures and high flow velocities in the areas where afterburning is triggered, validation of theoretical values of these two parameters by experiments presents serious technical difficulties.

It is easier, although somewhat uncertain, to validate theory by measuring effects induced using the methods described below.

3. Description of the Methods Used to Measure the Characteristics of the Plume and Smoke

The experimental methods developed have as a main objective the study of phenomena induced by the flow of the gas–particle mixture of the plume and smoke.

Firings generally take place on static benches, and projecting the measurement values to the real case of a missile in flight involves risky extrapolation. The static test results therefore most often serve to classify the propellants tested for the optical phenomenon under study. Greatly different results may occur in flight, as predictable with appropriate computer programs.

3.1. MEASUREMENT OF THE RADAR ATTENUATION

The presence of alkaline or alkaline-earth metal vapors, often just as traces (a few tens of ppm) in the combustion gases, causes significant ionization of the medium when the temperature is sufficiently high ($T > 2000$ K). This situation occurs in the combustion chamber of the rocket motor and in the afterburning region of the plume.

Free electrons subjected to the excitation of a radar wave with a frequency of several gigahertz traversing the medium begin to vibrate. A portion of the energy picked up is later dissipated in the plume through collisions with the more massive gas molecules in the plume (N_2, such as HCl, O_2). The energy lost from the wave, known as attenuation, is measured in decibels, using the formula:

$$A = -10 \log \frac{I_r}{I_e}$$

where I_e is the intensity of the incident wave and I_r the residual intensity of the wave after absorption by the plume.

The attenuation value depends not only on the frequency of the radar wave, but also on the characteristics of the ionized medium traversed (electronic density, collision frequency, etc.) [5].

For the purpose of simply comparing propellants, the attenuation is usually measured transversely (that is perpendicular) to the axis (Fig. 4). This measurement is not directly comparable with the measurements obtained by a control station when the missile is in flight. For this reason a second type of

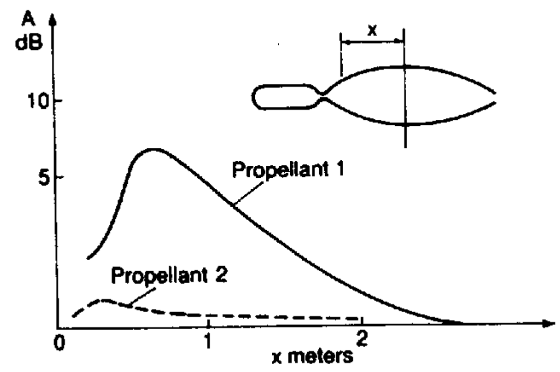

FIG. 5.4. Attenuation measured perpendicularly to the axis of a rocket motor for two different propellants.

device is used to measure the attenuation as a function of the sighting or aspect angle θ (Fig. 5), known as a longitudinal or diagonal measurement.

For any specific propellant there usually is a ratio of 6 to 10 between the maxima of attenuation obtained by longitudinal and transverse methods unless the plume electron density is so high that non-linear effects, such as refraction and diffraction, modify the longitudinally measured radiation.

3.2. OPTICAL TRANSMISSION IN THE VISIBLE AND INFRARED RANGES

As examples, two methods of measurements used to study the optical phenomena related to the occurence of smoke will be described:

- measurement made with a "smoke meter";
- measurement on a free plume.

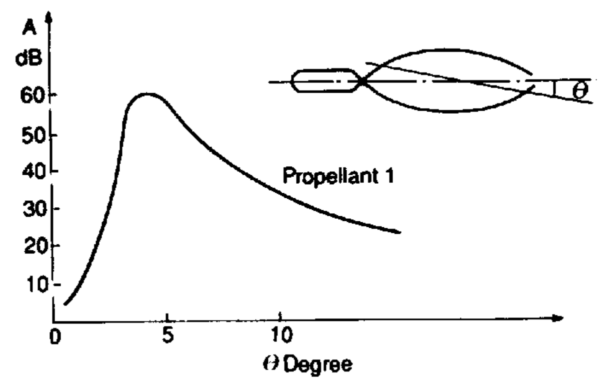

FIG. 5.5. Attenuation measured longitudinally.

3.2.1. *The smoke meter*

The smoke meter is a subsonic wind tunnel, 10 m long and 1 m in diameter, in which static motor firings are made to compare various propellants under standard conditions by measuring the transparency of their primary smokes. The optical measurements are made at the exit of the wind tunnel (Fig. 6), with dilution of the exhaust flow between 10^{-1} and 10^{-2} expressed by the ratio of the respective flow rates of the motors and the air drawn into the wind tunnel.

The major drawback is that the device is not very representative of the real conditions under which smoke is formed. Furthermore, it does not allow the study of firing with a short burning time (less than 2 s). But the measurements are little influenced by the perturbations of outside climatic conditions, and therefore are easily reproduced.

3.2.2. *Free jet measurements*

The test site for free jet firings must be protected from wind, and be sufficiently spacious so as not to disturb the shape of the smoke trail.

A stationary measurement of the transmission is made, perpendicular to the axis of the trail, in an area located downstream from the exit plane where all primary smokes are usually condensed. A non-stationary (source and sensor moving parallel to the trail axis) measurement allows estimation of the rate of build-up, settling, and dissipation of the smoke trail behind the motor of a missile versus time. A longitudinal measurement may be made instead.

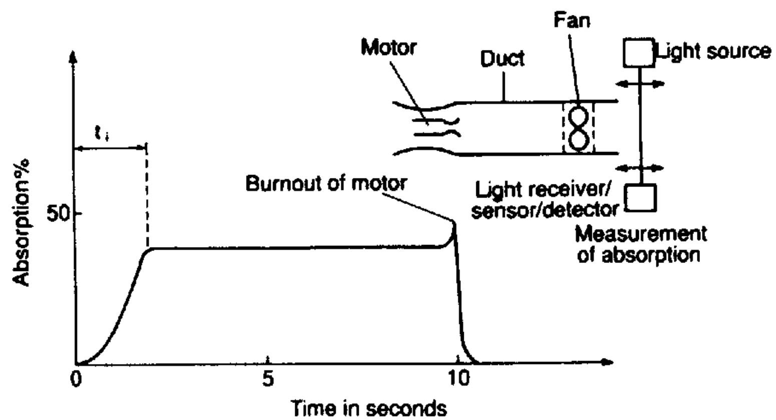

FIG. 5.6. Absorption measurement at exit of smoke measurement device. (t_i) is the time needed to reach a stationary flow in the duct).

3.2.3. *Optical instruments*

The instruments used to measure the transmission, through the smoke trail, consist of an emitting source and a detector. The transmission level is given as the ratio of the intensity received by the detector during the firing to that before or after the firing.

The selection of the source and the detector depends on the range of wavelengths in which the measurements are to be made. The range is always located within the limits where the atmosphere is transparent.

3.3. MEASUREMENT OF INFRARED EMISSION BY A PLUME

The plume of a rocket motor is a source of heat, similar to an infinite number of point sources emitting a radiation characteristic of the temperature and of the local concentration of chemical products, either gaseous or condensed.

The resulting total emission is not the sum of the point sources because for each emitting point a portion of the radiation is partially absorbed or scattered by the other points in the vicinity.

The emission spectrum of a plume, whose maximum intensity is in the short to mid-infrared wavelengths, is the superposition of a continuum of particle radiation and radiation manifesting the vibration-rotation or rotation-only types of radiation transfer (emission, absorption and scattering) phenomena, of the gas molecules thermally excited.

An increase in the temperature in a plume, and chemical changes of the mixture such as occur with afterburning, cause a corresponding increase of the total intensity and a change in the spectrum of the radiation.

The use of an infrared camera (thermal imager) has allowed assessment of afterburning; in particular, the verification of the efficiency of some flash suppressors compounds in a smokeless propellant, by comparing the intensity radiated by the plume from a modified propellant composition to that of a propellant containing no such additive.

4. Description of the Methods of Analysis

The modeling of the physicochemical phenomena occurring downstream of the exit plane of the nozzle required the development of computer programs to simulate both the flow and chemistry of the gas-particle mixture, and the optical phenomena tied to the plume or the smoke trail.

4.1. THE FLOW PROGRAMS

4.1.1. *Analysis of the flow of a plume*

The results of the analyses of the properties of a plume depend on the simplifying assumptions used to solve the Navier-Stokes equations, as well as on the types of measurements on which the comparisons with theory are based. Two types of models and computer programs are generally used when there is a possibility of afterburning.

In the zone close to the base of the missile where there is a confluence of the nozzle flow and the flow of external air behind the nozzle exit plane, and up to a distance of 10 nozzle radii, the program used will calculate the three characteristics (Fig. 7): pressure, temperature and velocity, as well as the chemical composition. This program can be used for the large pressure gradients that occur in this region. To reduce computer run times, simplified chemical reaction schemes are often used; for example, use of reactions involving only five gaseous products (CO, CO_2, H_2, H_2O, O_2) is often adequate.

Further from the nozzle exit plane, a satisfactory description of the plume can be obtained by using a computer program [6] assuming a constant pressure in the plume, thereby allowing the use of a more sophisticated set of chemical reactions. In particular, it is accepted that, in spite of the notorious imprecision of some values of the rate constants in reactions that give rise to free radicals, only a flow model using a chemical reaction system, such as the system recommended by Jensen [7], affords the possibility of correctly assessing the afterburning phenomenon [8]. More complex computer programs calculate pressure fluctuations of the plume with a full reaction set [9].

The ability to predict the plume with a computer program is fairly limited in the case of weak afterburning [10,11]. The discrepancy between the computer model and reality is probably related to imprecisions in the kinetic model used in the computer programs, as well as to the fact that the fluctuations due to turbulence are not taken into account in the calculations of the chemical reactions in the plume. These two points are currently the subject of many studies.

4.1.2. *Analysis of a flow in a smoke trail*

Much further downstream from the nozzle exit plane, the combustion products have cooled down, the gases are diluted, and all chemical products likely to condense in the ambient temperature form a trail of smoke which shows the flight trajectory of the missile. The trail of condensed water vapor left behind by a jet plane is caused by the same phenomenon.

A computer program can calculate temporal evolutions of the temperature, the velocity, and the dilution in each location of the trajectory, taking into

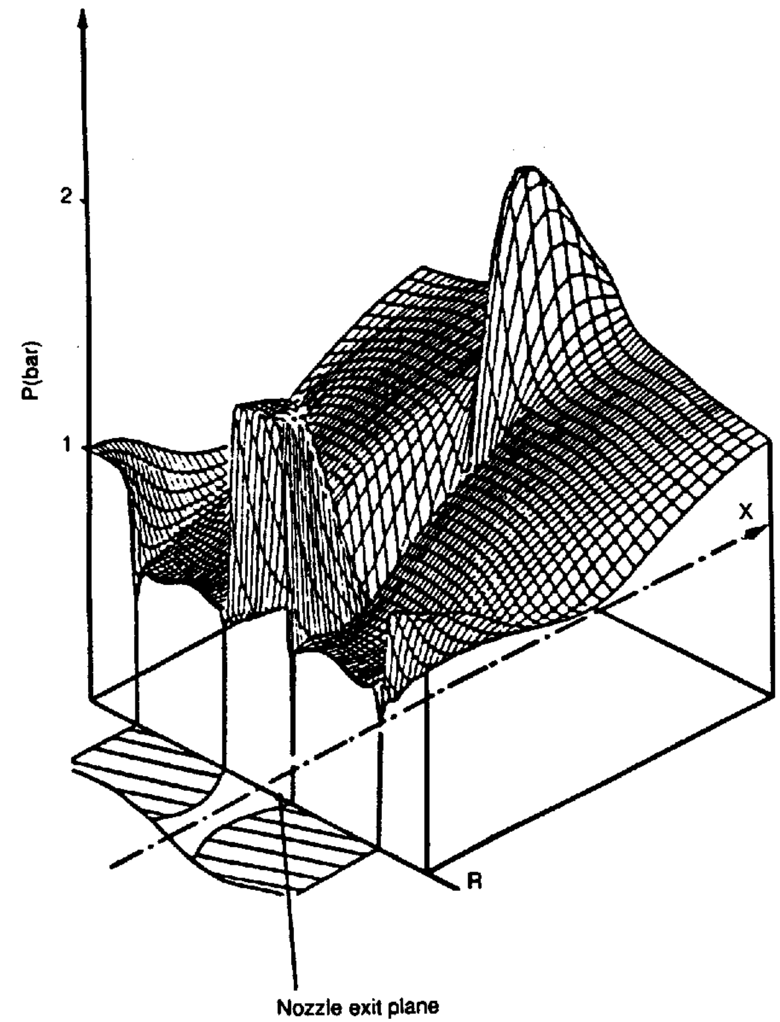

FIG. 5.7. Pressure field in a plume..

account the flight characteristics of the missile (direction, speed), the atmospheric conditions affecting the rapidity with which the trail dissipates (wind velocity, ambient temperature), and the characteristics of the residual products ejected by the nozzle (temperature, velocity, condensable fraction).

As an example, the modeling of the smoke trail may be based on the one-dimensional flow, using an empirical law of dilution of the combustion gases with the air along a specific trajectory of a missile [12]. The input data include the velocity, the temperature and the composition of the gases and size and number distribution of particles exiting the nozzle.

4.2. THE OPTICAL PROGRAMS

Calculations of physical values such as the emission, absorption, transmission, and visible, infrared or radar scattering, is done using computer programs whose input data are specific to the phenomenon being studied, and use the results obtained with the flow programs described in Section 4.1.

4.2.1. *Calculation of radar attenuation*

Absorption is the major cause of radar attenuation. On the line-of-sight of the radar link that intercepts the plume, the attenuation is the sum of the local discrete values of absorption expressed in decibels/cm according to:

$$\alpha = 0,08686\left(\frac{\omega}{c}\right)\left[-\frac{1-A}{2}+\frac{1}{2}\sqrt{(1-A)^2+A^2\left(\frac{\vartheta}{\omega}\right)^2}\right]^{1/2}$$

where $A = \omega_p^2/(\vartheta^2 + \omega^2)$ and $\omega_p^2 = 3.181 \times 10^3\, n_c$ (rad/s)^2

ω, ϑ, ω_p and n_c representing, respectively, the signal frequency, collision frequency, plasma frequency and local electronic concentration of the plasma environment. The signal frequency data are supplied by the missile designer; the other data are obtained by calculations of the plume flowfield, using the computer programs in Section 4.1.1.

Refraction, diffraction, and scattering are phenomena that are often neglected, but may be very important in operational situations with high electron concentrations in the plume. The effect of diffraction is to change the polar distribution of radar energy in the far field of the plume. The result is that the maximum attenuation (signal loss) value may be much less than would be caused by line-of-sight absorption alone [5,13]. Refraction and diffraction by the plume may also cause guidance errors by ducting around the plume radar energy to and from the target, with a resulting shift in the apparent target location.

Another radar interference effect is manifested as noise on the radar carrier frequency, presumably due to scattering of the radar wave by large refractive index gradients associated with high-velocity turbulent eddies in the plume. This noise can interfere with and mask missile control information coded into the radar wave [14-16]. The same scattering phenomenon causes backscatter of the radar wave, manifested as the plume radar cross-section.

4.2.2. *Calculation of optical transmission*

According to the Beer-Lambert law, the transmission factor is expressed by:

$$T = e^{-(N\sigma_a + N\sigma_d)Z}$$

with

$$\sigma_a = \frac{Q_a}{\pi r_0^2} \text{ and } \sigma_d = \frac{Q_d}{\pi r_0^2}$$

N, r_0, σ_a, σ_d are, respectively, the number of particles in the environment, their average radius, the effective absorption and scattering cross-section, and Z, the thickness of the medium traversed.

Q_a and Q_d are complex functions that provide the values of the absorption and scattering coefficients, as a function of the optical refractive index n of the particles, their radius, and the wavelength lambda of the signal. Electron microscope measurements of the diameter of particles from samples taken from the plumes and smoke trails of motors with variable flow rates resulted in particle sizes ranging from 1/100 μm to several tens of μm.

The theory of scattering of light [17,18], enables us to calculate the various Q_d for each of the following three cases:

(1) where the radius of the particle is small in comparison with the wavelength (Rayleigh scattering);
(2) where the radius of the particle and the wavelength are similar (Mie theory);
(3) where the radius of the particles is very large in comparison with the wavelength (the domain of geometrical optics).

Because the calculations in the Mie range are complex, a computer program [19] is used to obtain the Q_a and Q_d coefficients for a population of particles (in this reference, obeying a log-normal law of particle size distribution). The last calculation to determine the light intensity scattered in all directions θ by this cloud of particles is done according to:

$$I_\theta = \frac{I_0\lambda^2}{8}\frac{(I_1 + I_2)}{r_0^2\pi^2}$$

with

$$I_i = \frac{\pi^2 r_0^2}{\lambda^2} Q_d P_i$$

P_i = the function values tabulated by Deirmendjian [20].

The calculations of the coefficients of transmission through primary smokes, based on experimental data on the nature and the size of the particles ejected by the nozzle, provide a certain amount of useful guidelines for the design of rocket propulsion propellants:

- Carbon soots are highly absorbing, regardless of the wavelength.
- As a rule, as long as the radius of the particles is not too great, transmission in infrared is usually better than transmission in the visible range.

- The scattering indices of copper and carbon are fairly similar. Both are high in terms of the signature of the plumes and smoke trails. Figure 8 shows, based on the size of the particles ejected by the nozzle, the maximum mass fraction for a number of materials that cannot be exceeded in order to keep a transmission through a given smoke trail (1 m thick, 5×10^{-2} dilution) equal to at least 95%.

We observe that only a very small amount of carbon is required to degrade the transmission in infrared at 10.6 μm, and that zirconium oxide is found to be better than aluminum oxide in the visible range.

4.2.3. Calculation of infrared emission

The first models for infrared emissions in plumes appeared in 1967, in the work of Rochelle [21]. They were followed by the NASA models and Lockheed in 1973, Aerodyne in 1974, and finally Grumman in 1976 [22]. In

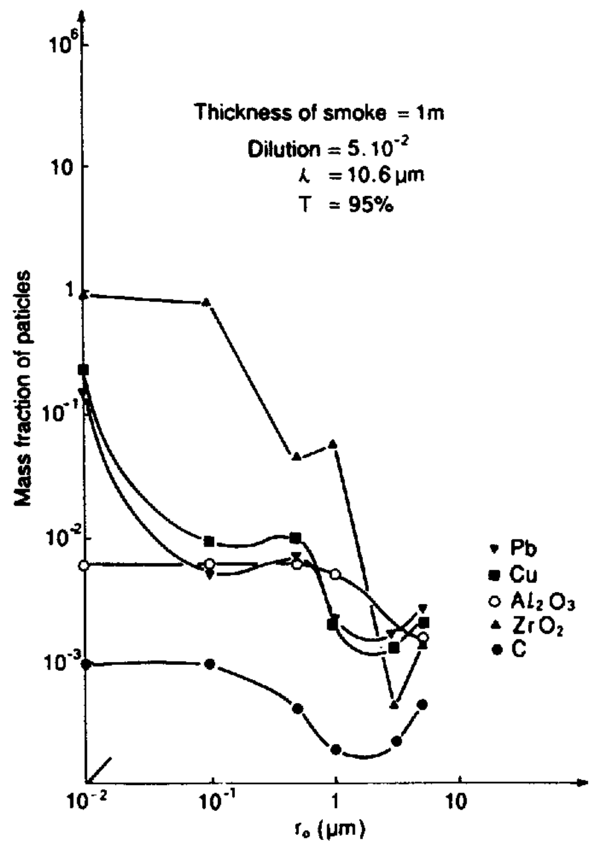

FIG. 5.8. Influence of the type, density and the radius of the particles, on the infrared transmission at 10.6 μm.

1978 the JANNAF Exhaust Plume Technology Subcommittee undertook to develop a standard model that included a standard plume flow model (SPF), and a standard infrared radiation model (SIRRM) [23].

A typical simple model calculates the infrared radiation of a gas particle mixture containing the main gaseous products (H_2O, CO_2, CO, HCl) and one condensed species, alumina.

Results from calculations of the infrared radiation in the plume of a motor burning aluminized propellant show that the infrared radiation is highest in the afterburning region, and in its absence it is highest just behind the first Mach disk.

4.3. PREDICTION MODEL FOR THE OCCURRENCE OF SECONDARY SMOKE

Under specific temperature and humidity conditions, atmospheric water vapor may condense into pure water drops and create fog. The combustion of a propellant containing ammonium perchlorate leads to the mixing of hydrochloric acid and water vapors. At a given temperature, and in the presence of an azeotrope, the saturating vapor pressure of the mixture is lower than that of pure water. This phenomenon results in condensation and the formation of a secondary smoke trail in the operational range when such propellants are used [24,25].

For a given temperature and humidity level, the quantity of condensed water versus the dilution ratio of the combustion products in the air can be determined. The mixing of these two vapors is assumed to be homogeneous, without any chemical reaction, and its enthalpy assumed equal to the sum of their total enthalpies. The conditions of thermodynamic equilbrium liquid/vapor are calculated from tabulated experimental data. Two possibilities emerge:

- the results of the calculations indicate that a complete lack of condensation is expected regardless of the dilution ratio of the combustion products in the air: secondary smoke will never occur;
- the results of the calculations indicate that there is a dilution ratio for which condensation is possible: this means there is a possibility that secondary smoke will form.

The results are plotted for each propellant, in a curve of the type shown on Fig. 2, that provides the minimum humidity level versus the ambient temperature of the air above which secondary smoke may occur.

5. Influence of Propellant Formulation on Transparency and Low Signature

At the start of a new program for a tactical or strategic missile, based on the requirements of the missile manufacturer for transmission on through the plume and low plume or trail signature, the propellant designer is often led to make a selection of the various ingredients that can be part of the formulation.

5.1. FLASH SUPPRESSORS

The addition of potassium salts in the formulation of homogeneous EDB and CDB propellants and Nitramites with high energy binder and HMX or RDX makes it possible to suppress the afterburning. Because these additives, for the most part, generate primary smoke, their percentage in the so-called smokeless propellants, as described in Table 3, must be limited to the exact amount required.

5.2. PARAMETERS AFFECTING THE RADAR TRANSMISSION

In composite propellants the K (potassium) equivalent content (K equivalent ≈ ppm of K + ppm × 1/10 of Na) is usually between 15 and 300 ppm. In homogeneous or Nitramite propellants, containing no ballistic additives, the level is often between 5 and 30 ppm.

Potassium in composite propellants is an impurity contained in the ammonium perchlorate, and in homogeneous or Nitramite propellants, an impurity contained in the nitrocellulose.

The K content of some insulation materials may reach 5000 ppm.

When there is afterburning in the plume, these amounts may cause very high levels of transverse attenuation (see Table 4) and unacceptably high signal loss in flight.

Other specific additives included in composite propellants exhibit anti-attenuation characteristics (tin, chromium or lead molybdenum). The mechanism of their action in the plumes remains, for the time being, rather poorly defined. It is thought, however, that they have the power to inhibit the occurrence of the OH radicals that initiate the afterburning.

TABLE 3 *Classification of the propellants[a] based on their signature*

Class	Primary smoke	Secondary smoke	Restrictions place on the formulation
Smokeless	Very little	None	No aluminum No AP Very low level of condensable species
Minimal smoke	Very little	Low density and not frequent	Little or no aluminum, Little AP(< 20%) Very low level of condensables species
Reduced smoke	Little	Yes	AP permitted Very low level of condensable species
High signature	Yes	Yes	None

[a] This classification cannot yet be considered as an international classification.
A working group of NATO/AGARD is now trying to define a standard international classification.

5.3. PARAMETERS AFFECTING THE PRIMARY SMOKE

Propellant metal fillers included as fuels, ballistic burning rate modifiers, and the metal fillers of the insulation materials included as additives to improve their heat resistance and structural integrity, are the main sources of primary smoke.

Consequently, a compromise must be sought between the increased plume signature and the gain in impulse due, for example, to aluminum.

Tests with a smoke meter show that the transmission in the visible range through smoke produced by an 82% ammonium perchlorate Butalane drops from 80% to 11% when the percentage of aluminum is from 0.5% to 8% (rocket motor flow rate around 500 g/s).

The same type of measurements performed at $\lambda = 2\ \mu m$ give two corresponding transmission values of 95% and 30%.

Aluminum-free propellants, in spite of the possible presence of ballistic additives, usually exhibit a very high level of transmission in the visible and infrared ranges. To avoid degrading these qualities it becomes necessary to optimize the nature and content of anti-instability additives included in the formulation, particularly in the case of radial burning, and to use an inhibitor producing little smoke for an end-burning propellant grain. In the last case, even when the best inhibitors are selected, the transmission drops by several percent. It is further necessary to optimize the igniter and the various rocket motor materials that come into contact with the combustion gases.

TABLE 4 *Transverse attenuation in a plume; function of the ratio of alkaline impurities*

Propellant	K Equivalent ppm	Afterburning	Attenuation dB	Frequency GHz
CDB	21	yes	16	10
Nitramite 1905 (minimum smoke CMDB)	150	yes	16	16
Nitramite 1903 (minimum smoke CMDB)	3720	no	0.2	16
EDB	2635	yes	11	16
Butalite (HTPB/AP)	45	no	1	10

5.4. PARAMETERS AFFECTING SECONDARY SMOKE

To obtain a total suppression of secondary smoke, on the ground and in a temperate climate, halogen, and therefore perchlorate, must be left completely out of the propellant. A very significant reduction in the frequency of occurrence and the opacity of the secondary smoke can be obtained—in Butalites—by limiting the proportion to less than 20%, as is the case for Nitramites G (see Section 2.4, above).

Bibliography

1. Carpentier, R., Le Guidage des missiles tactiques. Bilan et évolution pour les années 90. Armement No. 84, 16-38, 1985.
2. Ramsay, D. A., The evolution of radar guidance. *GEC J. Res.*, 3(2), 92-103, 1985.
3. Jarman, R. T. and Turville, C. M., The visibility and length of chimney plumes. *Atmos. Environ.* 3, 257-280, 1969.
4. Jensen, D. E., Prediction of soot formation rates: a new approach. *Proc. Roy. Soc. London, Series A*, 338-375-396, 1974.
5. Victor, A. C., Plume signal interference. Part 1, Radar attenuation. NWC China Lake. California. NWC TP 5319 Part 1, 1975.
6. Mikatarian, R. R., Kaw, C. J. and Pergament, H. S. Air Force Rocket Propulsion Laboratory. A fast computer program for non-equilibrium rocket plume predictions. Aerochem Research Laboratories AD 751984 Aerochem-TP-282; AFRPL-TR-72-94. August 1972.
7. Jensen, D. E. and Jones, G. A., Reaction rates coefficients for flame calculations. *Combust. Flame*, 32, 1-34, 1978.
8. Prigent, G. and Dervaux, M., Prédiction de l'atténuation électromagnétique de propergols solides composites. Processus de combustion et de détonation. ICT Internationale Jahrestagung, Karlsruhe, 713-728, June 1979.
9. Dash, S. M., Analysis of exhaust plumes and their interaction with missile airframes. *Tactical Missile Aerodynamics*. Progress in Astronautics and Aeronautics, Vol. 106, AIAA, New York. 1986.
10. Mace, A. C. H., Exhaust signature predictions for rocket motors. AGARD Conference Proceedings No. 391 (Confidential) Smokeless Propellants, 1985.
11. Ajdari, E., Méthodologies et moyen d'étude de la discrétion des moteurs à propergols solides. AGARD Conference Proceedings No. 391 (Confidential). Smokeless Propellants, 1985.
12. Victor, A. C. and Breil, S. H., A simple method for predicting rocket exhaust smoke visibility. *Spacecraft J. Rockets*, 14(9), 526-533, 1977.
13. Senol, A. J. and Romine, G. L., Three-dimensional refraction/diffraction of electromagnetic waves through rocket exhaust plumes. *Spacecraft J. Rockets*, 23(1), 39-46. 1986.
14. Victor, A. C., Plume signal interference. Part 2, Plume-induced noise. NWC, China Lake, California. NWC TP 5319 Part 2, 1972.
15. Williams H., Wilson A. S., and Blake C. C. Scattering from a Turbulent Rocket-Exhaust Jet Illuminated by a Plane Wave. *Electron. Lett.*, 7(19), 595-597, 1971.
16. Clarricoats, P., Seng, L. M., Travers B. and Williams, H., Scattering from a turbulent rocket-exhaust jet illuminated by a focused microwave beam. *ibid*, pp 597-600.
17. Kerker, M., *The Scattering of Light and Other Electromagnetic Radiation*. Academic Press, New York, 1969.
18. Van Der Hulst., *Light Scattering by Small Particles*. John Wiley and Sons, New York, 1967.
19. Grehan, G., Gouesbet, G. and Rabasse, C., The computer program SUPERMIDI for Lorenz MIE theory and the research of one to one relationship for particule sizing. ISL-R-117, 1980.
20. Deirmendjian, D. *Electromagnetic Scattering on Spherical Polydispersions*. American Elsevier, New York, 1969.

21. Rochelle, W. C., Review of thermal radiation from liquid and solid propellant rocket exhaust. N.67.31300. NASA-TM. 53579, 1967.
22. Vanderbilt, D. and Slack, M., A model for emission and scattering of infrared radiation from homogeneous combustion gases and particles. Grumman Research, AD-A027 576/8. Department Memorandum RM-621, 1976.
23. Ludwig, C. B., Malkmus, W., Walker, J., Slack, M. and Reed, R., The Standard Infrared Radiation Model A-81-039063. American Institute of Aeronautics and Astronautics, Thermophysics Conference. (U.S.), Vol. 16, pp 81-1051, 1981.
24. Miller, E., Smokeless propellants. *Fundamentals of Solid Propellant Combustion*. Progress in Astronautics and Aeronautics, Vol. 90, AIAA, New York, 1984.
25. Victor, A. C., Computer codes for predicting the formation of rocket exhaust secondary smoke in free jets and smoke chambers. NWC, China Lake, California. NWC TM 3361, 1978.